

# SIMULATION OF COAL COMBUSTION PROCESS IN SMALL BOILER

Radovan Nosek<sup>1</sup>, Jozef Jandacka<sup>1</sup>, Andrzej Szlek<sup>2</sup>

<sup>1</sup>University of Zilina, Univerzitna 8215/1, 010 26 Zilina, Slovakia

<sup>2</sup>Silesian University of Technology. Konarskiego 22, 44-101 Gliwice, Poland

Emails: [radovan.nosek@fstroj.uniza.sk](mailto:radovan.nosek@fstroj.uniza.sk), [jozef.jandacka@fstroj.uniza.sk](mailto:jozef.jandacka@fstroj.uniza.sk), [andrzej.szlek@polsl.pl](mailto:andrzej.szlek@polsl.pl)

Received January 2011, Revised March 2011, Accepted April 2011

## Abstract

The aim of the work is to develop a method of simple characterization of solid fuels combustion in fixed bed, which would be useful for CFD modelling. In this work, the measurements were performed in a test rig, where a combustion front propagates against the airflow. Concentrations of flue gas species were registered at the exit of a fixed bed reactor and the temperature of burning coal was measured in selected points of the reactor as functions of time. Furthermore, developed functions were applied for defining the boundary conditions at the interface between the fixed bed and gas phase using FLUENT. The simulations of a domestic boiler have been done and the relative effects of different factors in CFD code were evaluated by sensitivity analysis.

**Keywords:** fixed bed reactor, coal, function, measurements, simulation, boiler

## 1. Introduction

Nowadays combustion provides more than 90% of the energy needs. Half of Europe's electricity is produced from fossil fuels and about 30% from the total is generated from coal, in Poland it is about 90%. Many countries use coal as a source of domestic and commercial heating requirements covering by fixed bed combustion of solid fuels. Transport of the fuel in the bed differs between boilers. Primary air passes through a fixed bed, in which drying, gasification, and charcoal combustion takes place. The aim of the work was to do series of measurements in fixed bed reactor, work out obtained results in a form of approximation function and develop a model of combustion of a fixed fuel bed on a grate and to compare the result from the model with measurements data from a test rig.

In the work of E. Widmann et al. [1] a model for NO<sub>x</sub> formation in biomass fixed bed furnace was developed. The model consists of an empirical biomass combustion model in the furnace and CFD-based NO<sub>x</sub> postprocessor based on a basic combustion simulation and a subsequent calculation of NO<sub>x</sub> formation.

The empirical model was applied for the combustion of the solid biomass fuel on the grate and the model parameters were based on batch reactor experiments. The transfer of obtained results from experiments to the combustion of a biomass fuel layer on a grate is valid if diffusion transport and mixing effects in the direction of the grate can be neglected compared to the transport

of the fuel along the grate. Although this condition is not fulfilled in general due to mixing effects on the grate, in their work the approach was adopted as a first experimental approximation.

The objective of the work of Yin et al. [2] is to present a reliable baseline CFD model for a thermal 108 MW biomass-fired grate boiler, which can be used for diagnosis and optimization of this boiler and the design of new grate boilers. In their work a sensitivity analysis was done on the basis of the design conditions of the boiler in order to evaluate the influence of different factors in CFD modelling of grate boilers. The purpose of the sensitivity analysis is to define the factors (the effects of meshes, models for the fuel bed, turbulence, and combustion) that may be important for modelling of biomass-fired grate boilers.

## 2. Description of measurement in the reactor

The measurements were performed in a fixed bed reactor (diameter 4.5cm, height 20cm), where a batch of coal was placed on a grate. The combustion air was fed from the bottom and bed was ignited from a top. The coal moves downward under the power of gravity in the course of the combustion process, counter - current to the combustion air. The counter - current process is the most common fixed bed coal combustion and gasification process.

Inside the reactor four thermocouples were installed in order to measure the temperature of burning coal in different heights. During the experiments the coal temperature was recorded on line in periods of 30 seconds by data logger. Thermocouples are located 50 mm apart from one to another. Concentrations of the flue gas species CO<sub>2</sub>, CO, O<sub>2</sub> and NO were registered by an analyser every 30 seconds. The initial temperature of fuel and inlet air is 298 K. Each test was repeated three times. Coal with a granularity of 1-30 mm, and a lower calorific value of 28 MJ/kg was used as a fuel.

The speed of the combustion front was calculated from the distance between thermo-couples placed on different heights in the reactor, and time meanwhile temperature of one thermo-couple reach the same value of temperature in the next one:

$$w = \frac{\Delta x}{\Delta t} \quad (1)$$

Where

$w$  - is propagation velocity of the combustion front through the fixed fuel bed (m/s)

$\Delta x$  - distance between each thermo-couple (m)

$\Delta t$  - time difference (s)

The resulting average velocity obtained from the calculation was in order of 0.1 mm/s (6 mm/min).

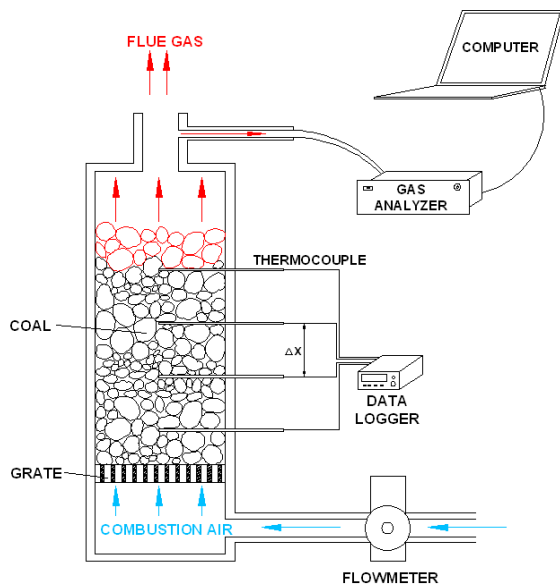


Fig. 1: The measurement setup with fixed bed reactor

### 3. Results of measurements

Figures 2 and 3 present an example of measured gas compositions at the outlet of the reactor. The gas compositions are given as mole fractions of the gas components. The fuel ignition is followed by propagation of a reaction front downward in the bed against the air flow. As the front passes, the fuel is heated, resulting in drying and devolatilization. Volatile gases are ignited and together with the char formed they burn as long as there is oxygen available, providing heat for propagation of the front.

In a large particle, exposed to a high heating rate, the drying and devolatilization fronts will closely follow each other, while in a small particle, drying is fully completed before devolatilization starts.

It can be noticed that two phases of combustion process can be distinguished (see Figures 2 and 3). Transition of first phase to second is dedicated to the carbon concentration decline in flue gas. The char burns to carbon monoxide and carbon dioxide, in the presence of oxygen. It causes very low oxygen concentration in the first phase of combustion process, while in the second it increases. The behaviour of carbon dioxide profile is opposite to the behaviour of oxygen, meaning that most of the time the concentration of it is high and in the second period decreases. Unstable concentration of CO in the first period is caused by poor mixing of fuel with air. The profiles of carbon monoxide and carbon dioxide decline when most of the char is burnout.

### 4. Approximation functions

Authors decided to use functions to describe the simplified profile of emissions formation. Functions were used in order to avoid random fluctuations as well as for determination of coefficients to evaluate emissions for intermediate values of airflow. The Method of Least Squares is in our case used for specification of coefficients. This method is a procedure, requiring just some calculus and linear algebra, to determine what the 'best fit' line is to the experimental data.

Copyright © 2011/gjto

The idea is to create a function with assumed linearity in the first part and in the second part assumed exponential decrease in the case of CO<sub>2</sub> and increase in the case of O<sub>2</sub> (see Figure 5).

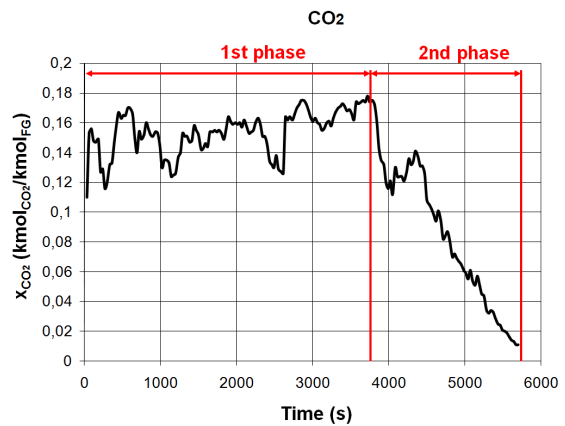


Fig. 2: Mole fraction of carbon dioxide at the exit of fixed bed reactor

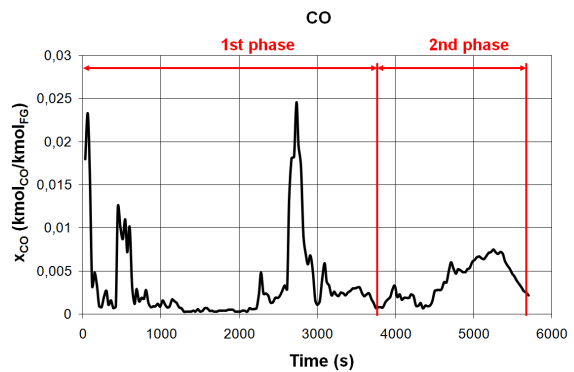


Fig. 3: Mole fraction of carbon monoxide at the exit of fixed bed reactor

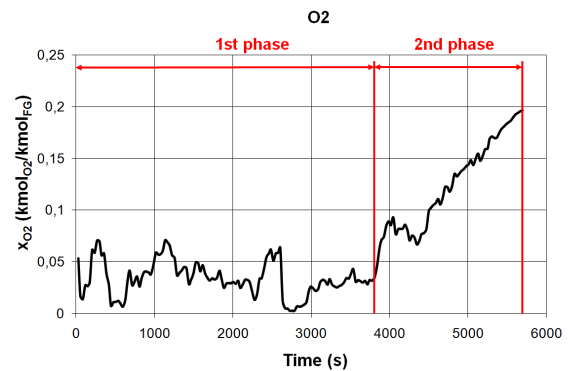


Fig. 4: Mole fraction of oxygen in flue gases

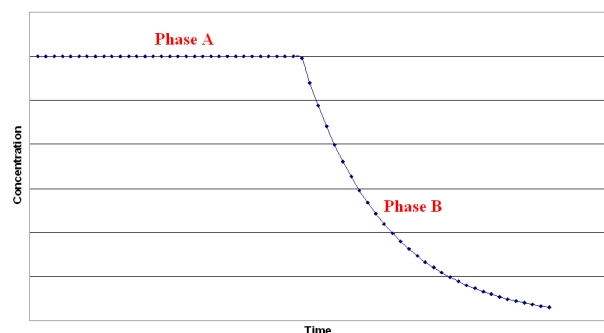


Fig. 5: Example of developed function (probable profile of CO<sub>2</sub> and temperature)

Developed functions are farther used for defining the boundary conditions at the interface between fixed bed and gas phase in FLUENT.

Author decided to approximate  $CO_2/O_2$ ,  $CO_2/CO$ ,  $O_2/CO_2$ ,  $O_2/CO$ ,  $CO/O_2$  and  $CO/CO_2$  ratios instead of  $CO_2$ ,  $CO$ ,  $O_2$  since it was observed that these ratios are characterized by small fluctuation. In the followed section the way of calculating emissions from functions is described.

#### 4.1. Phase A

The phase A is in our case considered as the steady course and the function of it is linear. The experimental results were converted in two approximation functions. A general form of these linear functions is:

$$x_A = A_{1A} + B_{1A}t \quad y_A = A_{2A} + B_{2A}t \quad (2)$$

where  $x_A=CO/CO_2$ , values of carbon monoxide and carbon dioxide are obtained from experimental results,  $y_A=O_2/CO_2$ , it is ratio of oxygen and carbon dioxide, t- is time (s). The Least Squares Method (LSM) was used for calculation of constants  $A_{1A,2A}$  and  $B_{1A,2A}$ .

Basing on above presented functions and mass balance a flue gas composition from the bed can be calculated.

Oxygen balance can be written as:

$$[O_2]: n'_a 0,21 + \dot{p} \left( \frac{n}{4} + \frac{moisture}{36} \right) = n''_{FG} \left( [CO_2] + \frac{1}{2} [CO] + [O_2] \right) \quad (3)$$

where  $n'_a$  is molar flow rate of air (kmol/s),  $n''_{FG}$  molar flow rate of flue gas (kmol/s) and  $\dot{p}$  is fuel consumption (kg/s). For the phase B the hydrogen and moisture can be neglected in this equation.

The fuel consumption is defined as:

$$\dot{p} = w \cdot \rho \cdot A \quad (4)$$

where w (m/s) is the propagation velocity of the combustion front through the reactor,  $\rho$  (kg/m<sup>3</sup>) is density of coal and A (m<sup>2</sup>) is area of grate in the reactor While nitrogen balance (assuming that N in a fuel is neglectable):

$$[N_2]: n'_a 0,79 = n''_{FG} (1 - [CO_2] - [CO] - [O_2]) \quad (5)$$

These three equations (3, 4 and 5) content three unknown parameters; so then  $CO_2$ ,  $CO$  and  $O_2$  can be expressed and calculated from these equations.

The relative error was applied to evaluate the results of measured and calculated data. The calculated average relative error in the case of carbon dioxide is 8.7 percent, average error of carbon monoxide is 37.6 percent and oxygen average error is 36.4 percent. The values of oxygen and carbon monoxide errors are acceptable.

#### 4.2. Phase B

Two approximation functions for phase B were worked out from obtained results using LSM. The first is exponential function of  $CO_2/CO$ , the second is  $O_2/CO_2$  and general forms of functions are:

$$x_B = A_{1B} e^{B_{1B}t} \quad y_B = A_{2B} e^{B_{2B}t} \quad (6)$$

where  $x_B=CO/CO_2$ ,  $y_B=O_2/CO_2$ , t- is time (s) and constants  $A_{1B,2B}$ ,  $B_{1B,2B}$  are calculated by LSM:

$$B_1 = \frac{\sum_{i=1}^n (x_{B0}^* t_i - x_{Bi}^* t_i + x_{Bi}^* t_0 - x_{B0}^* t_0)}{\sum_{i=1}^n (t_i^2 - 2t_i t_0 + t_0^2)} \quad (7)$$

$$B_2 = \frac{\sum_{i=1}^n (-y_{B0}^* t_i + y_{Bi}^* t_i - y_{Bi}^* t_0 + y_{B0}^* t_0)}{\sum_{i=1}^n (t_i^2 - 2t_i t_0 + t_0^2)} \quad (8)$$

Where:

$$x_{B0}^* = \ln x_{B0} \quad y_{B0}^* = \ln y_{B0} \quad (9)$$

$$x_{Bi}^* = \ln x_{Bi} \quad y_{Bi}^* = \ln y_{Bi} \quad (10)$$

and

$$A_{1B}^* = x_{B0}^* + B_{1B} t_0 \quad (11)$$

$$A_{2B}^* = y_{B0}^* - B_{2B} t_0 \quad (12)$$

$$A_{1B} = e^{A_{1B}^*} \quad A_{2B} = e^{A_{2B}^*} \quad (13)$$

where n - number of experimental values;  $x_0$ ,  $y_0$ ,  $t_0$  - are initial values of phase B. In order to obtain continuous function (phase A and B), approximation of phase B was done in such a way that calculated  $x_A$  is equal to  $x_0$  in a moment of transit.

Knowing approximation functions, an amount of  $CO_2$ ,  $O_2$  and  $CO$  emissions can be computed using the equations (3) to (5). In figures 6 to 8 the calculated and measured concentration profiles are compared to each other.

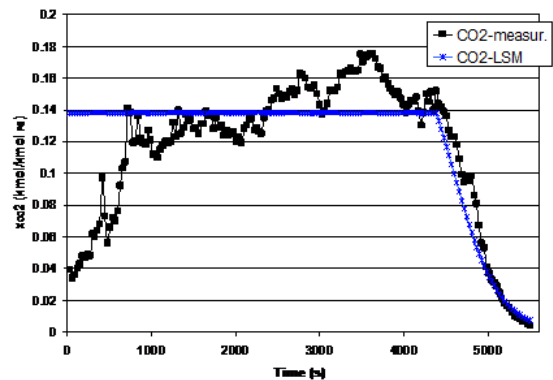


Figure 6: Comparison of carbon dioxide between results of test and its function

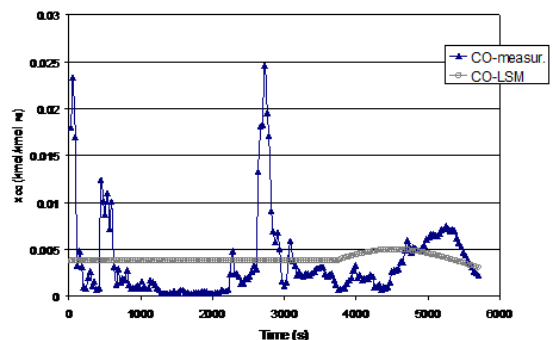


Figure 7: Comparison of carbon monoxide between results of test and its function

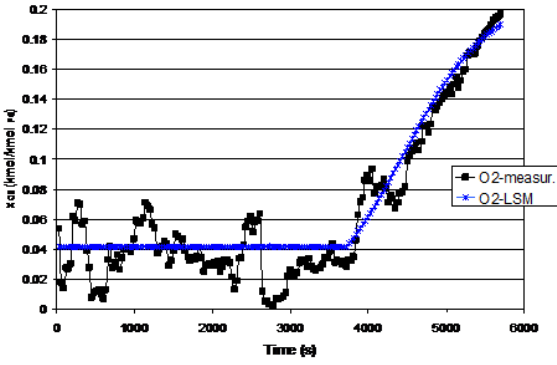


Figure 8: Comparison of oxygen between results of test and its function

Levels of coupling between experimental and computed values were formulated by the correlation coefficient. Correlation coefficient value of measured carbon dioxide and computed  $CO_2$  is 0.74. The correlation between oxygen from the tests and calculated is 0.95, and carbon monoxide correlation coefficient is 0.52. The formation of CO is sensitive to the changes (downward movement of coal under gravity, presence of oxygen) which occur during combustion process. All of these factors can be reason of low carbon monoxide correlation coefficient.

The correlation coefficient is always between -1 and +1. The closer the correlation is to +/-1, the closer to a perfect linear relationship. The correlations indicate a high level of association between measured and computed values.

## 5. CFD model

In this section the models used for the simulation are described. These models supply mass flux, species concentrations and temperatures of the flue gases above the surface of the fuel layer as boundary conditions for the subsequent CFD simulation of the turbulent reactive flow.

CFD is based on solving conservation or transport equations for mass, momentum, energy and chemical species. The basic equations for a fluid in turbulent flow are the Reynolds-averaged Navier-Stokes (RANS) equations and the forms of them for steady state are defined as follow:

### Continuity equation

The gas phase conservation equation of mass is written as:

$$\nabla(\bar{\rho v}) = 0 \quad (14)$$

where  $\rho$  ( $kg/m^3$ ) is density of the fluid and  $\bar{V}$  (m/s) is its ensemble-averaged velocity vector defined on a 3D domain.

### Momentum conservation equation

The Navier-Stokes is the momentum conservation equation and is defined as:

$$\frac{\partial}{\partial x_j}(\rho U_i U_j) = -\frac{\partial p}{\partial x_i} + \frac{\partial \tau_{ij}}{\partial x_j} + \rho f_i \quad (15)$$

where  $p$  (Pa) is the static pressure,  $f_i$  are the sum of external forces and  $\tau_{ij}$  ( $N/m^2$ ) is the viscous stress tensor and is described by the Newton law:

$$\tau_{ij} = \mu \left( \frac{\partial U_i}{\partial x_j} + \frac{\partial U_j}{\partial x_i} \right) - \frac{2}{3} \mu \delta_{ij} \frac{\partial U_l}{\partial x_l} \quad (16)$$

where  $\delta_{ij}$  is the Kronecker symbol and  $\mu$  ( $kg \cdot m^{-1} \cdot s^{-1}$ ) is the molecular viscosity, depending on the fluid properties.

### Energy conservation equation

When considering heat transfer within the fluid or solid regions of the domain, Fluent also covers the energy equation. This equation is written below in general form:

$$\frac{\partial}{\partial x_i}(\rho h U_i) - \tau_{ij} \frac{\partial U_i}{\partial x_j} + \frac{\partial q_i}{\partial x_i} = \rho U_i f_i + S_h \quad (17)$$

where  $S_h$  includes the heat of chemical reaction,  $h$  (J) is the total specific enthalpy and for a multicomponent medium takes the following form:

$$h = \sum Y_i h_i \quad (18)$$

where  $Y_i$  is the mass fraction of species  $i$  in the mixture and  $h_i$  is the total enthalpy written as:

$$h_i = h_{T_{ref},i}^0 + \int_{T_{ref}}^T C_{p_i}(T) dt \quad (19)$$

where  $h^0$  is the enthalpy of formation,  $T_{ref}$  (K) is the reference temperature and  $c_{p_i}$  ( $J \cdot kg^{-1} \cdot K^{-1}$ ) is the specific heat at constant pressure.

### Species transport equation

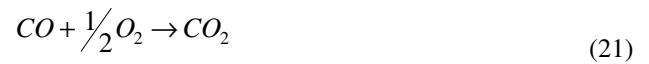
Finally, the behaviour of the species is solved by the following equation:

$$\nabla(\rho \bar{v} Y_i) = -\nabla \bar{J}_i + R_i + S_i \quad (20)$$

where  $S_i$  ( $kg \cdot m^{-3} \cdot s^{-1}$ ) is the rate of creation by addition from the dispersed phase plus any user-defined sources,  $R_i$  ( $mol \cdot m^{-3} \cdot s^{-1}$ ) is the mass rate of production or depletion by chemical reaction and  $\bar{J}_i$  ( $mol \cdot m^{-2} \cdot s^{-1}$ ) is the molecular diffusion flux of species  $i$ . Fluent applies the finite volume method to solve the governing flow equations described above.

### Combustion model

The relevant gas-phase reactions in combustion are assumed to be normally fast. The Eddy Dissipation Model (EDM) the effective reaction rate is employed above the fuel bed, where the temperature is high and the kinetics of the reactions is fast enough to be considered instantaneous, leading to a combustion process that is entirely controlled by the mixing of fuel species with oxygen. On the other hand, near the walls and water pipes, where the temperature of the gases is suddenly reduced, mixing may be strong, but it is also necessary to account for the kinetic control. The combustion scheme of the combustion employed in this work is presented in equation:



The model used for numerical prediction supports following settings as boundary conditions for the subsequent CFD simulation of the turbulent reactive flow: velocity, species concentrations and temperatures of the flue gases above the surface of the fuel layer. Simulation of the combustion process usually requires large computational efforts involving high grid densities, especially in the regions where higher gradients are expected. High numbers of equations regarding combustion

chemistry have to be solved in order to capture combustion and heat transfer details taking place inside the system [3].

Boiler geometry is one of the critical stages in CFD simulation; proper definition of the geometry provides a more realistic scenario for the simulation. In the domain just half of the combustion chamber has been modelled, taking advantage of the symmetry. For the grid sensitivity analysis, two grids were constructed and run in FLUENT to determine a grid density and quality that was fine enough to obtain a solution of acceptable accuracy. The two meshes whose results are presented in this thesis are as follows:

**Mesh-I:** An unstructured tetrahedral mesh with about 330,000 cells. It may be the traditional mesh scheme used for the modelling of the boiler because such a mesh can be generated in the short time and the computational cost is low (Figure 9).

**Mesh-II:** A hybrid hexahedral mesh created by dividing the boiler geometry into several small, individual sections or volumes and meshing them separately. It is a high-quality mesh consisting of 400,000 cells. Finer cells are employed where the main gradients are expected. The geometry of the boiler was modified in order to generate hexahedral mesh in the region of retort burner and deflector (Figure 10).

The most important part of the work was the determination of the detailed boundary conditions. At the inlet of retort following boundary conditions were set: profiles of calculated concentrations ( $\text{CO}$ ,  $\text{O}_2$ ,  $\text{CO}_2$  and  $\text{H}_2\text{O}$ ), temperature and velocity of flue gases. Boiler walls and pipes were set at temperature 343 K and symmetric plane as symmetry.

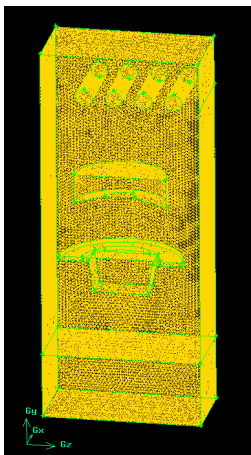


Fig. 9: Boiler geometry - Unstructured grid

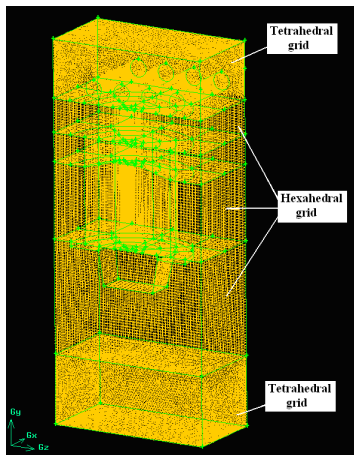


Fig. 10: Modified geometry of the - hybrid grid

The modelling of the turbulent reactive flow in this work is based on the *Standard  $k-\epsilon$*  Turbulent Model, the Discrete Ordinates Radiation Model and the Eddy Dissipation Model (turbulent gas phase combustion). The sensitivity of turbulence model to CFD predictions is also evaluated. In the calculations the following turbulence models have been used:

Turbulence:

- the *standard  $k-\epsilon$*  model
- the *realizable  $k-\epsilon$*  model
- the *RNG  $k-\epsilon$*  model

## 6. Measurements of the domestic boiler

The investigated boiler is designed for operation in domestic central heating system. The numerical predictions were verified by the experimental data obtained from small boiler.

Short description of the Boiler- SAG: Rated heat power -25kW. The fuel from the container at the boiler side is transferred by the

automatically controlled feeding screw to a furnace by retort stoker. The screw warrants an uninterrupted operation and the rotary retort burner ensures that no burnt fuel in the form of ash is moved down to the ash box.

The boiler construction was changed – in to the water coat exchanger was drilled several slots, so the probe could be easily inserted inside the combustion chamber during the tests (Fig.11). Emissions and temperature of flue gases were measured in the chamber as well as in the outlet of the boiler. First series of tests were carried out in the center of chamber and second series were done in the 10 cm far field region from the center (Fig.12). Temperature of water was measured during the test in the inlet and outlet of water pipes. Combustion Stoichiometry for fuel and Energy Balance of the boiler were calculated using measured data.

Results of measurements are evaluated for CFD simulations in following section.



Fig. 11: Test boiler

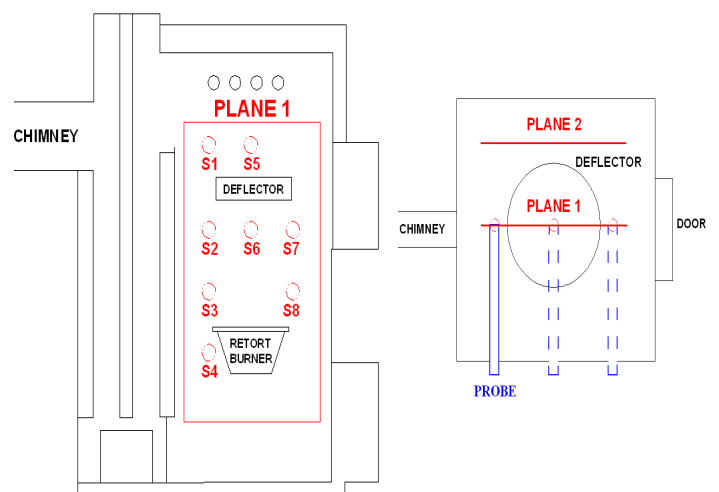


Fig. 12: Positions of measurement performed in the chamber (slot 1-8)

## 7. Results

In this section, the results of the numerical simulations are presented and compared with measured values from boiler.

*Comparison of measured and calculated results - first plane (centre) in the combustion chamber*

The flue gas temperature field is indicated in Fig.13. Computed temperature from selected position is shown in Fig.14. The numerical predictions of temperature are in very good agreement with the measured values.

In Fig.15 the numerical predictions of CO<sub>2</sub> are compared to data from measurements. It is important to note that calculated concentrations in the region of the deflector (slots 2, 6 and 7) are in the range of the experimental results. The predicted values are in very good agreement with measured data.

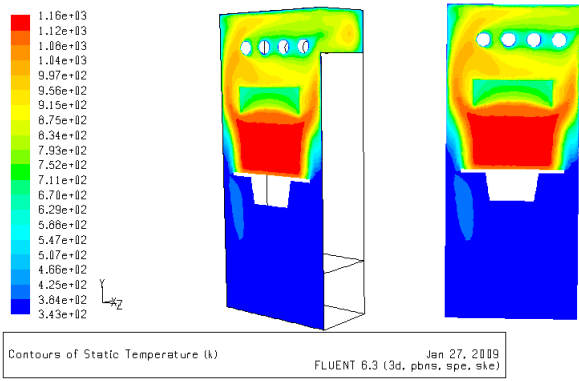


Fig. 13: Flue gas temperature field in the centre of combustion chamber

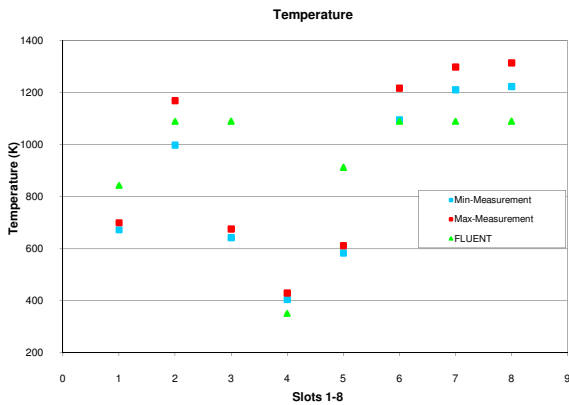


Fig.14: Comparison of measured and calculated temperature

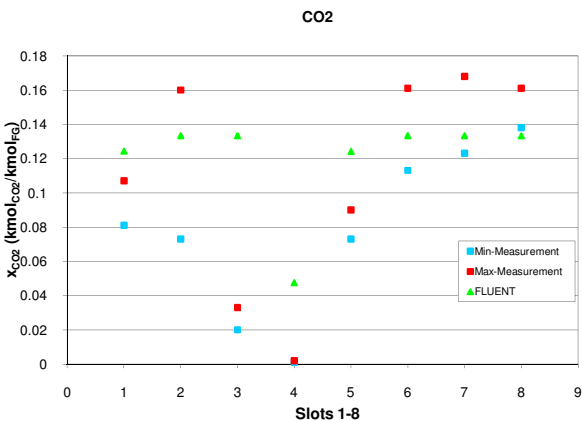


Fig.15: Comparison of measured and calculated carbon dioxide

Carbon monoxide concentrations are illustrated in Fig.16 and 17. The results of CO were divided in two graphs due to high concentrations in slots 2, 6, 7. The low concentrations of generated CO in the gases are estimated by the model and a maximum concentration of about 0.01 % is calculated in slots 3 and 8. Numerical values are in acceptable agreement with measured CO.

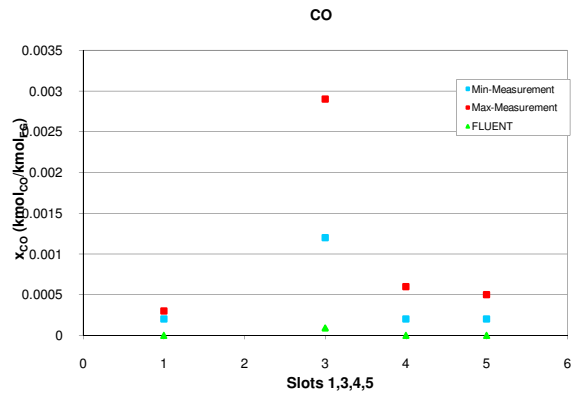


Fig.16: Comparison of measured and calculated carbon monoxide (for slots 1,3,4,5)

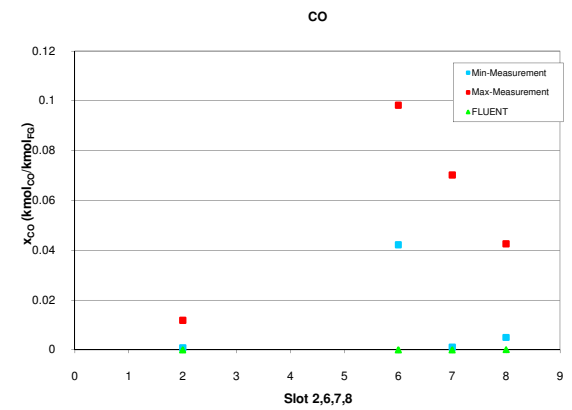


Fig.17: Comparison of measured and calculated carbon monoxide (for slots 2,6,7,)

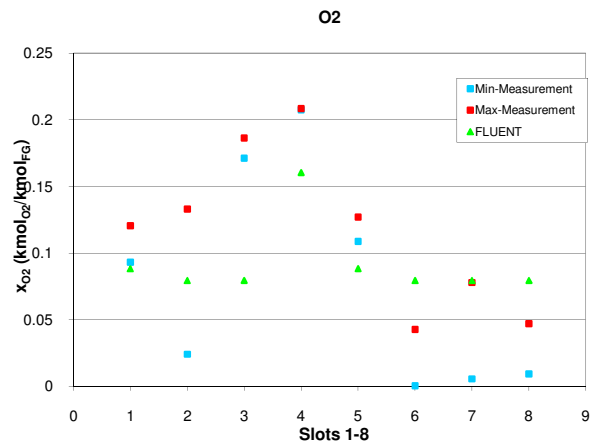


Fig.18: Comparison of measured and calculated oxygen

In Fig.18 the oxygen concentrations are shown. No major differences between the measurements and calculated values can be observed. Low value of average relative error 0.52% was computed.

*Comparison of applied meshes*

The purpose of this section is to evaluate the factors that may be important in the modelling of the domestic boiler. The results of sensitivity analysis are presented below.

The comparison of CO<sub>2</sub> concentrations shows that two applied meshes gave different results where the high quality grid (mesh II) indicates better agreement with experiments. The model with mesh I over predicted the formation of carbon dioxide. In the case of oxygen, the results of finer mesh (mesh II) gave a more accurate prediction (see Figure 19 and 20).

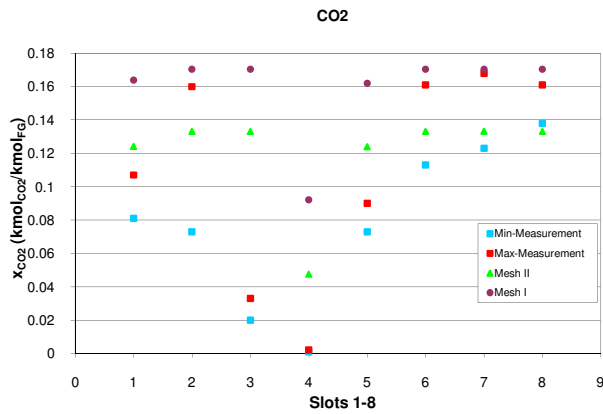


Fig.19: Comparison of carbon dioxide in certain points of combustion chamber

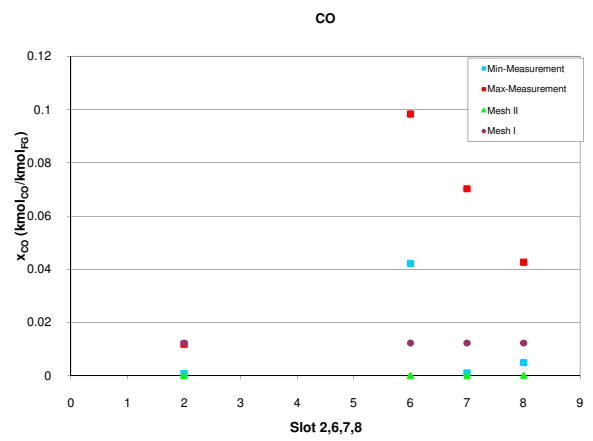


Fig.22: Comparison of predicted carbon monoxide

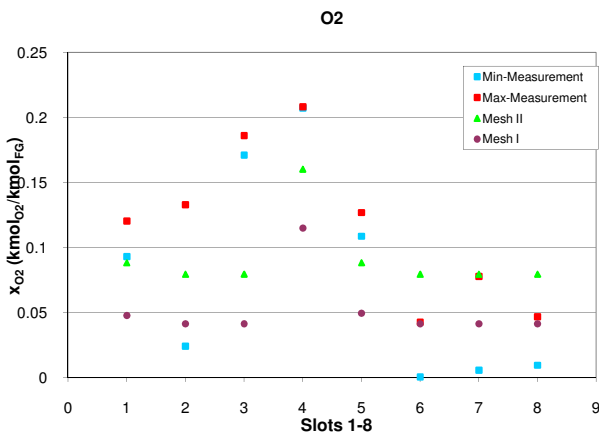


Fig.20: Comparison of oxygen in certain points of combustion chamber

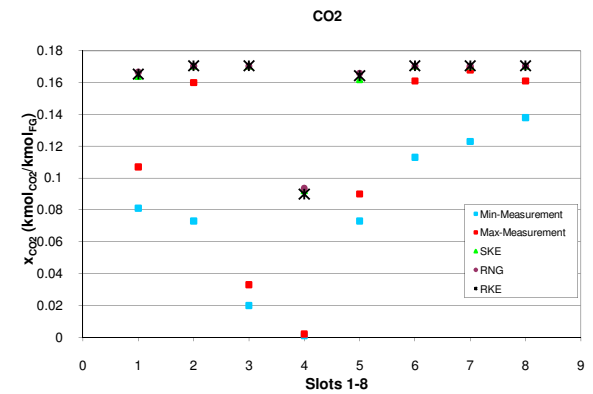


Fig.23: Comparison of carbon dioxide in certain points of combustion chamber

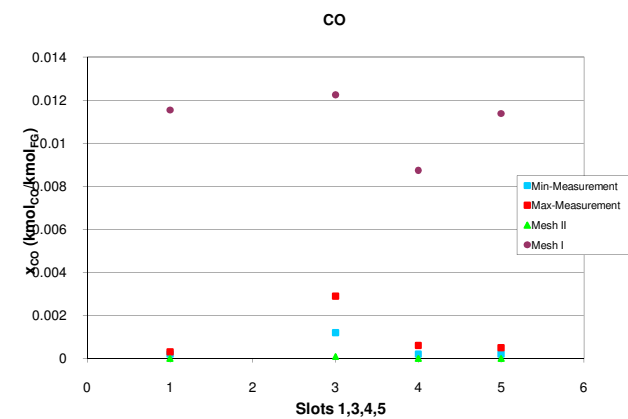


Fig.21: Comparison of predicted carbon monoxide

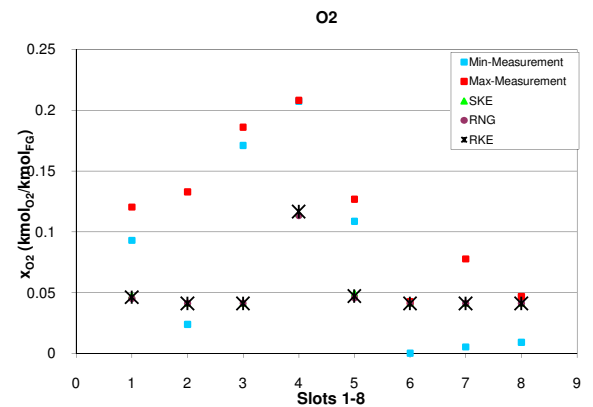


Fig.24: Comparison of oxygen in certain points of combustion chamber

Figures 21 and 22 show the effect of varying the grid quality on the predicted generation of carbon monoxide. The results computed by the unstructured grid exceed measured data in slots 1,3,4 and 5, but in the region of main combustion process are in good agreement with experiments. It was determined that the results calculated using mesh II gave very low concentrations of CO and these results were in worse agreement with measurements.

Different mesh schemes affect the accuracy of the solution and in the case of mesh II can be noticed higher accuracy of the CFD results.

*Comparison of turbulence models*

The three turbulence models considered in this study were used to simulate the gas species and temperature.

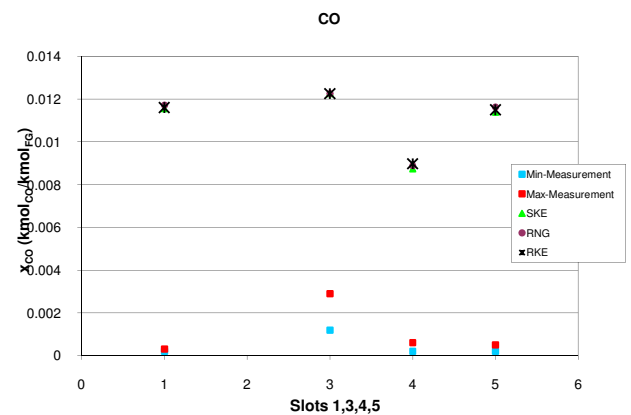


Fig.25: Comparison of predicted carbon monoxide

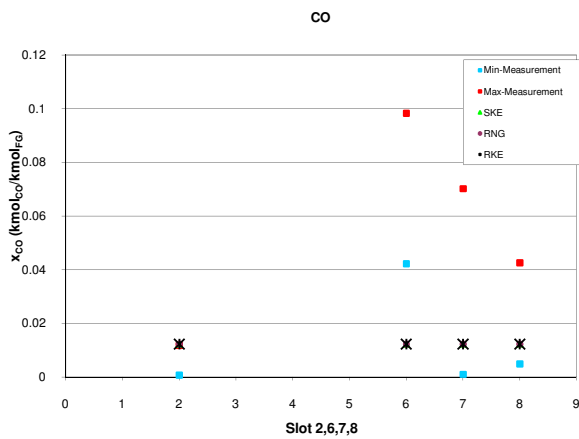


Fig.26: Comparison of predicted carbon monoxide

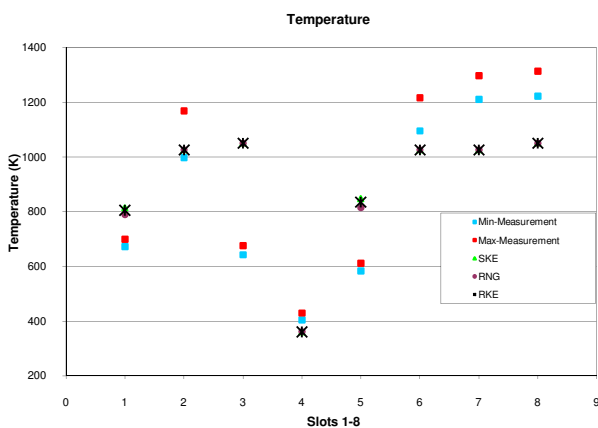


Fig.27: Comparison of predicted and measured temperatures

The realizable and standard models are very similar with slightly different dissipation ( $\varepsilon$ ) equation as well as in the way of calculating the eddy viscosity ( $C_{\mu}$ ). The difference of results obtained with these two models is negligible, as can be seen from Figures 23 to 27.

The RNG model gave results comparable to those obtained using the standard and realizable  $k$ - $\varepsilon$  models. The main difference between the RNG and standard model is in the equation of the turbulent viscosity. The RNG calculates the effect of swirl on turbulence more accurately and therefore is better for swirling flows.

## 8. Conclusions

The aim of this thesis was to develop a method of simple characterization of solid fuels combustion in fixed bed with emphasis placed on  $\text{CO}_2$ ,  $\text{CO}$  and  $\text{O}_2$  formation. The development of the method was based on experiments in a fixed bed reactor, approximation of obtained results, mathematical modelling and verification of the model by measurements collected in a domestic boiler. The goal was to examine whether the self-developed empirical model could predict the characteristics of coal combustion.

Considering all uncertainties of measurements in a fixed bed reactor which underlie fluctuations in operation conditions, the qualitative agreement with the calculations is satisfactory.

Functions describing the formation of  $\text{CO}_2$ ,  $\text{O}_2$  and  $\text{CO}$  in fixed bed combustion were compared with measurements. The comparison shows that the computed carbon monoxide and oxygen with measured profile have intense association and it is

nearly identical in the second part of combustion process (phase B). Carbon dioxide obtained from calculation has a good relationship with experimental data. However, the comparison indicates that the functions catch the principle combustion behaviour of the carbon dioxide, oxygen and carbon monoxide generation.

A significant effort, in both modelling and experimentation, has been made toward a reliable CFD model for the 25 kW domestic boiler. Gas temperature and composition were measured with a probe in order to evaluate the accuracy of predicted results by the model.

The numerical results indicate that the predicted generation of  $\text{CO}_2$  is consistent with the data measured in the centre plane (1.Plane). No major difference in the comparison of  $\text{O}_2$  concentrations was found and predictions agree reasonably well with the experiments. The numerical values show that formation of carbon monoxide was underestimated by the model. An overall reliable agreement was found in the comparison of predicted and measured temperature. More efforts are needed in the experimentation to provide reliable.

The reasonable discrepancies were thoroughly examined between *mesh-I* and *mesh-II*. The grid with higher quality provided results in better agreement with experiments. Mesh quality affects face – flux calculations between cells and therefore directly impacts the accuracy of the solution and the convergence. Besides the grid quality, grid density also plays important role since it determines how densely the discrete solutions are used to approximate the solutions. A mesh of high grid density and quality tends to improve the accuracy of numerical predictions.

All turbulence models applied in the simulations gave results for gas temperature and composition that were similar and comparable to the experimental results. The  $k$ - $\varepsilon$  Standard and  $k$ - $\varepsilon$  Realizable models provided a similar behaviour, while the  $k$ - $\varepsilon$  Standard model shows the closest results to the experimental data. The RNG turbulence model had the worst performance of all investigated models. The observed discrepancies can be attributed to the modelling of turbulent viscosity, Reynold stresses and the use of turbulent diffusion of  $k$  and  $\varepsilon$ .

From a modelling perspective, the main aim of simplifications, algorithms of solution, numerical models and methodology employed seem to be correct as the prediction of the main behaviour of the system has been made with an acceptable level of accuracy. The numerical results indicate that the predicted generation of  $\text{CO}_2$  is consistent with the data measured in the centre plane. No major difference in the comparison of  $\text{O}_2$  concentrations was found and predictions agree reasonably well with the experiments. The simulations indicated that the probable reason for low  $\text{CO}$  prediction is that most of the carbon monoxide is converted to carbon dioxide. More tests and comparisons with measurements are necessary in order to improve the model. Furthermore, the different CFD settings could lead to an improvement in pollutant formation and temperature distribution in the furnace.

The local discrepancies might quantify the effect of the differences in the boundary conditions used in the model and in the real model. The results of this work show that the use of a simplified model for the gas phase, coupled with the CFD simulations, can be applied for fixed bed boiler modelling.

## 9. Acknowledgements

This work has been supported by the European Commission in the context of the 6<sup>th</sup> Framework Programme (INSPIRE; Marie Curie Research Training Network, Contract No. MRTN-CT-2005-019296)

**10. References**

- [1] WIDMANN, E., SCHARLER, R., STUNBERGER, G., OTENBERGER, I. (2004). Release of NO<sub>x</sub> precursors from biomass fuel beds and application for CFD-based NO<sub>x</sub> postprocessing with detailed chemistry, 2nd World Conference and Exhibition on Biomass for Energy, Industry and Climate Protection, Rome, Italy.
- [2] YIN, CH., ROSENDAL, L., KAER, S.K., CLAUSEN, S., HVID S.L., and HILLE T. (2008). Mathematical Modeling and Experimental Study of Biomass Combustion in a Thermal 108 MW Grate-Fired Boiler, *Energy & Fuels*, Vol. 22, No. 2.
- [3] PORTEIRO J., COLLAZO J., PATINO D., GRANADA E., GONZALES J.C.M., MIGUEZ J.L., (2009) Modelling of a biomass pellet domestic boiler, *Energy & Fuels*, Vol.23..
- [4] LINDAU J., RÖNNBÄCK M., SAMUELSSON J., THUNMAN, H. LECKNER, B. (2002). An Estimation of the Spatial Resolution when Measuring Gas Concentrations Inside a Burning Fixed Bed', Presented at the Nordic Seminar – Thermo Chemical Conversion of Biofuels, Trondheim, Norway.
- [5] SMITH B. and RANADE J. (2003). Computational Fluid Dynamics for Designing Process Equipment: Expectations, Current Status, and Path Forward, *Ind. Eng. Chem. Res.*, vol.42, 1115-1128.
- [6] WILK R. K. (2002) Low emission Combustion, Wydawnictwo Politechniki Slaskiej, Gliwice.
- [7] IBLER, Z. (2002). Technicky pruvodce energetika. 1. dil - 1. vyd. - Praha : BEN.
- [8] LOWRY, H. H. (1945). Chemistry of Coal Utilization, John Wiley, New York.
- [9] FLUENT Inc. of ANSYS Inc. GAMBIT 2.2 Documentation (2006). User's Guide.
- [10] FLUENT Inc. of ANSYS Inc. FLUENT 6.3 Documentation. (2006). User's Guide.
- [11] LENHARD R. (2010). Numerical simulation device for the transport of geothermal heat with forced circulation of media, Fourth Global Conference on PCO 2010, Kuching – Sarawak - Malaysia.
- [12] HUZVAR J., JANDACKA J. (2010). Project of Micro Co-Generation Unit on Wood Pellets Combustion, *Archivum combustionis*, page. 445-450.
- [13] VASZI, Z., VARGA, A. (2009). Design and verification of the mathematical model for detecting the throughput of the compressor stations In: *Acta Metallurgica Slovaca, Slovakia*.